



HYDROGENATION OF TOLUENE ON Ni-Co-Mo SUPPORTED ZEOLITE CATALYSTS

S. M. Shuwa^{1,*}, B. Y. Jibril² and R. S. Al-Hajri³

^{1,2} CHEMICAL ENGINEERING DEPARTMENT, AHMADU BELLO UNIVERSITY, ZARIA, KADUNA STATE, NIGERIA

³ PETROLEUM AND CHEMICAL ENGR. DEPT., SULTAN QABOOS UNIVERSITY, P.O. BOX 33, PC 123, MUSCAT, OMAN

*E-mail addresses:*¹ smsuwa@yahoo.com, ² rashidh@squ.edu.om, ³ byjibril@gmail.com

ABSTRACT

Mixed oxides of Ni, Co and Mo supported on five zeolites -ZSM-5-a, ZSM-5-b, HY-a, HY-b and Mordenite were prepared and characterized using many techniques for use as hydrotreating catalysts. In a preliminary investigation, toluene was employed as model compound to test the catalysts in hydrogenation, as a major upgrading reaction. TGA/DSC analysis showed that the impregnation of the metals slightly affected the thermal stability of the zeolites with all catalytic samples displaying good stability up to 730°C. The XRD patterns for all the catalytic samples showed that the framework of the zeolites were retained after impregnation. XRD and TPR results confirmed the presence of molybdenum trioxide on the zeolites with NiCoMo/HY-b displaying high metal-support interaction due to low reduction temperatures. The activity results showed that toluene conversion of almost 100% and selectivity to mainly methyl-cyclohexane was achieved. The catalysts activity test showed that the zeolite support textural properties particularly surface area, pore volume and pore diameter affect the performance of the catalysts. NiCoMo/HY-b displayed the best performance after the few minutes of the reaction due to its high surface area, pore volume and average pore diameter.

Keywords: Hydro treating catalysts; Hydrogenation; Toluene conversion; Surface area; Pore diameter

1. INTRODUCTION

Catalysts, particularly noble metals have been used for decades in refineries to upgrade heavy oil fractions and residue. Metals often use are Pt, Pd, and Ru usually as a supported catalysts [1, 2]. Commonly use supports are silica, alumina and zeolites. Supported noble metals hydrogenation catalysts are highly expensive with high vulnerability to sulfur poisoning; this led to a declined interest in their use in a conventional hydrogenation process. Transition metals of group VI (Mo, W) are also reported to be effective hydrogenation catalyst [3-5]. They are less expensive and exhibit high resistance to sulfur poisoning. Metals like Ni, Co, Rh and Ru have been reported by many researchers to increase the hydrogenation ability of many hydrogenation/hydrocracking catalysts [6-11]. Takema-Wada *et al* investigated the synergistic effect between Ni and Pd loaded Y-type zeolite in HCK of polycyclic aromatics. The results showed that the Ni-Pd/Y catalyst has the highest activity toward the hydrocracking reactions of phenanthrene and pyrene among the catalysts employed [9]. In another work, the incorporation of Ru (0.5wt%) into a NiMo/Al₂O₃ catalyst was shown to

enhance the activity of the catalyst by about 30% at 673K [8].

Sato *et al* carried out HCK reactions of diphenylmethane and tetralin over three different types of zeolites (USY, HY and mordenite) with or without NiW sulfide, to establish the roles of catalytic bifunctionality [11]. Jessica *et al* prepared aluminosilicate-supported Pt-Ru for hydrogenation of toluene. When compared with their monometallic counterparts, the bimetallic catalysts displayed significantly high turnover frequencies due to the synergy between Pt and Ru. In another work involving a bimetallic catalyst system; zeolite-alumina composite supported NiMo catalyst was developed and used in hydro cracking of decalin and 1-methylnaphthalene [12]. To the best of our knowledge, no data are available on investigation of mixed oxides of Ni, Co and Mo on toluene hydrogenation reaction. There are still important questions regarding the effect of zeolite acidity, pore sizes and surface area on hydrogen insertion reactions. The role of the mixed metal oxides on the conversion and products distribution has not been categorically established. Therefore, the aim of this study was to prepare trimetallic zeolite-supported

* Corresponding author, tel.: +234-806-540-0736

catalyst based on mixed oxides of nickel, cobalt and molybdenum and investigate their performance in toluene hydrogenation.

2. EXPERIMENTAL

2.1 Catalyst Preparation

Five different zeolites were procured commercially from Zeolyst International and used as support materials in this work (Table 1). They are of the types; HY, ZSM-5 and Mordenite. A trimetallic catalyst containing nickel, cobalt and molybdenum were prepared from each support by co-impregnation with an aqueous solution containing all the metal precursor salts with a concentration to produce 20wt% total metal loadings. The concentration of each metal precursor solution was prepared in order to get the final loading in the catalyst to satisfy the atomic ratio: $Ni/(Ni + Co + Mo) = 0.3$ and $Mo/Co = 3$ [13]. The metal precursor salts used are nickel nitrate hexahydrate (99%, BDH), cobalt nitrate hexahydrate (99%, Merck) and ammonium heptamolybdate (99%, Fisher Scientific, $(NH_4)_6Mo_7O_{24} \cdot 4H_2O$) for nickel, cobalt and molybdenum respectively. The impregnated trimetallic catalysts were dried in air at 110°C overnight, calcined at 500°C for 4 hours.

2.2 Catalyst characterization

The catalytic samples obtained were characterized using the following techniques: The BET characterisation was obtained using a Tristar 3000 (Micromeritics) gas adsorption analyser, which can determine specific surface area along with average pore diameter and average pore volume. This was achieved by placing the sample under vacuum to degas, followed by flushing with helium gas for 2 (mins). The vacuum was then reintroduced to complete the degassing process. The sample was then subjected to varying pressures of nitrogen gas at liquid nitrogen temperature, and the absorption of nitrogen at these pressures was recorded to obtain an adsorption isotherm. Specific surface area was measured by using BET equation. Metal loading was determined using Inductive Coupling Plasma-Optical Emission Spectroscopy (ICP-OES). The sodium peroxide fusion method was adopted for the analysis. X-ray diffraction technique was used to identify the phases and determine size of the crystallites of the catalysts. Analysis was carried out using a PANalytical XpertPro, which operates at 40 kV and 40 mA. Xpert data viewer software was used in conjunction with the instrument. The scan was carried out between 2θ equal to 18.0° and 50.0°, with a step size of 0.02° and time per step of 99.695 ms.

Temperature programmed reductions (TPR) were also conducted using a Micromeritics AutoChem 2910 instrument, using approximately 100 mg of catalyst. Samples were held in a U-shaped tube and cooled to -50°C under a flow of Ar. The samples were reduced using 5% H_2 in Ar while the temperature was ramped ($10^\circ C \text{ min}^{-1}$) up to 800°C. Hydrogen uptake was monitored every minute by a thermal conductivity detector (TCD). Thermogravimetric analysis (TGA) and differential scanning calorimetry (DSC) were both conducted using a Metler Toledo instrument where samples were loaded in a ceramic crucible. For TGA, the TGA/DSC 1 star e system was used and ~10 mg of sample was heated to 800°C at a rate of $20^\circ C \text{ min}^{-1}$ in a flow of air. For DSC, a DSC 1 star e system was used ~10 mg was heated to 500°C with a rate of $20^\circ C \text{ min}^{-1}$ in a flow of N_2 .

2.3 Catalyst activity test

The catalytic performance evaluation for toluene hydrogenation was studied in Autoclave Engineers 100 mL-capacity mini batch reactor. The catalysts amount (0.1g) was loaded into the reactor containing 1 mL of toluene dissolved in 29 mL of dodecane (30 mL solution). The reaction was performed at a temperature of 200°C and total hydrogen pressure of 20 bar. All the catalytic samples (10 in number); including the zeolite supports were tested at that condition. Liquid samples were withdrawn every 30 mins for GC analysis. No gaseous samples were detected and taken for analysis. A Clarus 500 GC (Perking Elmer) was used for compositional analysis. The GC oven temperature was specified to achieve fast separation of the hydrocarbons: 80°C hold for 2min, to 200°C at $10^\circ C/\text{min}$ and hold for 10 min, to 300°C at $5^\circ C/\text{min}$ and hold for 20 min.

3. RESULTS AND DISCUSSION

3.1 Catalyst Characterization

3.1.1 Surface Area and Porosity

The specific surface area, pore volume and average pore diameter of the five zeolite supports used in this work are given in Table.1.

The porosity results from BET analysis shows that the zeolite materials used are micro-pores as their average pore diameter is less than 2 nm [14, 15]. It is also evident from Table 1 that pore volume of pores less than 1.14 nm of all the supports constitute about 40 to a little less than 50% of total pore volume. While pore volume of pores up to 28.1 nm constitute a little above 50% of the total pore volume of all the supports. This is

confirmed by the average pore diameters of the zeolite supports which range from 1.59-1.94 nm which is an indication that the sizes of most of the pores fall below 2 nm. This indicates that the zeolites are micropores and the implication is that only molecules with average kinetic diameters less than 2nm will be able to access internal pore structure of the zeolites.

Table.1 Textural properties of the zeolite supports

Sample	Si/Al ratio	Surface area (m ² /g)	pore volume (g/cm ³)		pore diameter (nm)
			<1.14nm	≤28.1nm	
ZSM-5-a	280	358.58	0.14	0.21	1.59
HY-a	80	601.34	0.25	0.42	1.64
Mordenite	20	389.72	0.18	0.72	1.87
HY-b	5.1	707.38	0.34	0.38	1.94
ZSM-5-b	50	356.30	0.15	0.22	1.65

Table 3: Metal Loadings of the Impregnated Catalysts

catalyst	metal atomic ratio {Ni/(Ni + Co + Mo)} theoretical actual	
	NiCoMo/ZSM-5-a	0.3
NiCoMo/HY-a	0.3	0.31
NiCoMo/Mord	0.3	0.33
NiCoMo/HY-b	0.3	0.37
NiCoMo/ZSM-5-b	0.3	0.38

Table.2 Textural properties of the impregnated catalyst samples

Sample	surface area, m ² /g	pore volume, g/cm ³		pore diameter, nm
		<1.14nm	≤28.1nm	
NiCoMo/ ZSM-5a	258.93	0.10	0.16	1.56
NiCoMo/HY-a	364.97	0.16	0.24	1.71
NiCoMo/Mord	208.70	0.09	0.14	1.77
NiCoMo/HY-b	302.16	0.14	0.17	1.89
NiCoMo/ZSM-5-b	246.87	0.10	0.16	1.67

Table 2 gives changes in the textural properties of the catalysts when impregnated on the supports to compare with the parent zeolite support samples as presented in Table 1. In all the catalysts, a reduction in surface area, pore volume and average pore diameter was noted when compared with zeolite supports.

The reduction is more pronounced in pores of sizes up to 28.1 nm than in pores less than 1.14 nm. This must have been the reason for slight reduction in average pore diameter since all the pore sizes are taken into consideration when computing its value. However, the decrease in pore diameter is very insignificant when compared with the decrease in pore volume, which indicates that the reduction in surface area is as a result of change in pore volume due to incorporation of the metals in the porous structure of the zeolite supports. The pore volume can reduce due to pore-filling of the supports by the respective metal species. Aggregation

of metal particles in the pore structure of the catalysts can also lead to reduction in pore volume[16]. Another reason that can lead to a decrease in surface area is reduction in external surface area due to the modification of the supports with the metals, since the BET technique encompasses external and pore area evaluations to determine total surface area. There is also a direct correlation between the decrease in surface area of the catalysts with respect to the supports and their pore diameters (Table 1 and Table 2). NiCoMo/HY-b has the largest pore diameter (1.94 nm) and also recorded the highest reduction in surface area (57%) while NiCoMo/ZSM-5-a with the smallest pore diameter (1.59) recorded the least reduction in surface area (28%) of all the supported catalysts. The reason is because large pore diameters will allow more access to the diffusing metal ions than small pore diameters in order to occupy the internal surface area. The occupation of the internal surface area by the metals (pore-filling) will lead to a reduction in its internal surface area which constitutes a greater proportion of total surface area of porous materials.

3.1.2 Elemental Analysis

The metal loadings of the catalysts were determined using inductive coupling plasma spectroscopy and the results are presented in Table 3.

There is clear deviation of the actual value measured by the ICP from the theoretical value (0.3) especially in NiCoMo/HY-b and NiMoCo/ZSM-5-b where the difference is around 0.07-0.08. Inhomogeneous distribution of catalyst precursors can lead to poor dispersion of the metals in the interior surface of the catalyst after calcining. This can lead to analyzing samples that are not true representatives of the catalytic samples.

In addition to that, high-calcining temperatures leads to loss in promoter atoms of the catalysts. At significantly higher temperature, the promoter ions tend to go subsurface (incipient spinel formation) and so are lost from surface, and eventually from the active phase [14]. Furthermore, molybdenum oxide (MoO₃) can undergo sublimation at higher temperature during calcining and can be lost from the system[17]. This might have been the case here as drop in molybdenum loading in NiCoMo/HY-b and NiCoMo/ZSM-5-b were observed which contributed to increase in the atomic ratios of the two catalysts.

3.1.3 X-ray diffraction (XRD)

XRD analysis was performed on all the five zeolite supports and the five catalytic samples from the

impregnated metals on the supports. The diffraction patterns for both samples are presented in Figures 1 and 2. The similarity of the XRD patterns between the parent supports and the impregnated catalyst samples indicates that the frameworks of the zeolite supports were retained after the impregnation process [1, 18-21]. Additional peak at $2\theta = 27.2$ was observed in all the supported catalyst samples. This peak is attributed to the presence of molybdenum trioxide (MoO_3) [16].

The crystal sizes of MoO_3 were estimated using Scherrer equation (equation 1).

$$D_c = \frac{K\lambda}{\beta \cos\theta} \quad (1)$$

In (1), D_c is the crystal size, K is the Scherrer constant (dimensional quantity) 0.9-1, 0.9 assumed here, λ is the X-ray wavelength, 0.197nm for $\text{Cu-K}\alpha$ radiation, β is the full width at half maximum height of the first peak in radians and θ is the diffraction angle (Bragg angle) in degrees

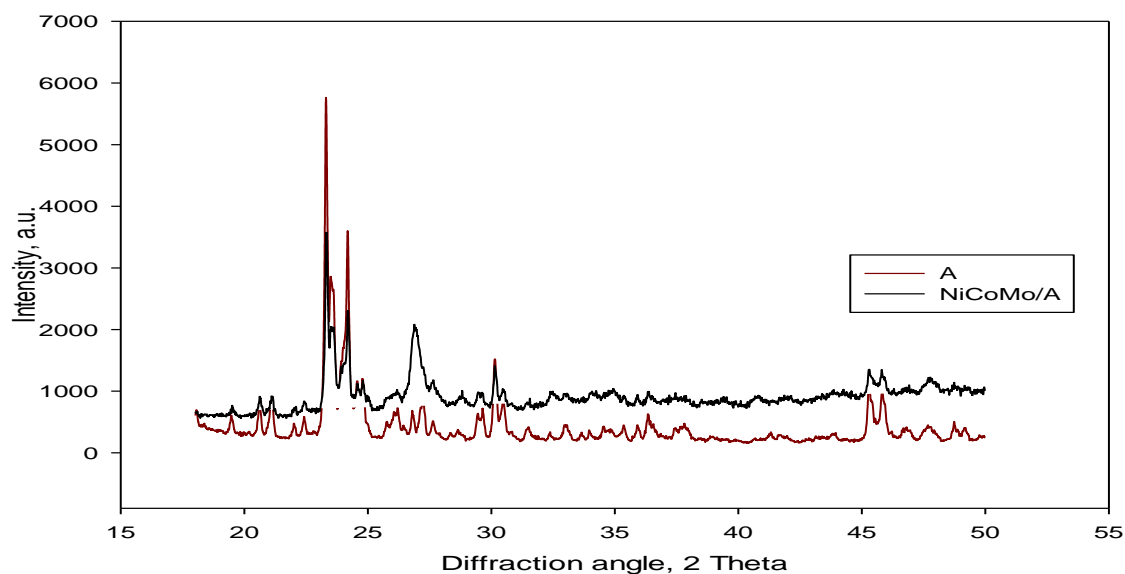


Fig.1: XRD patterns of samples NiCoMo/A and support A (A = ZSM-5a)

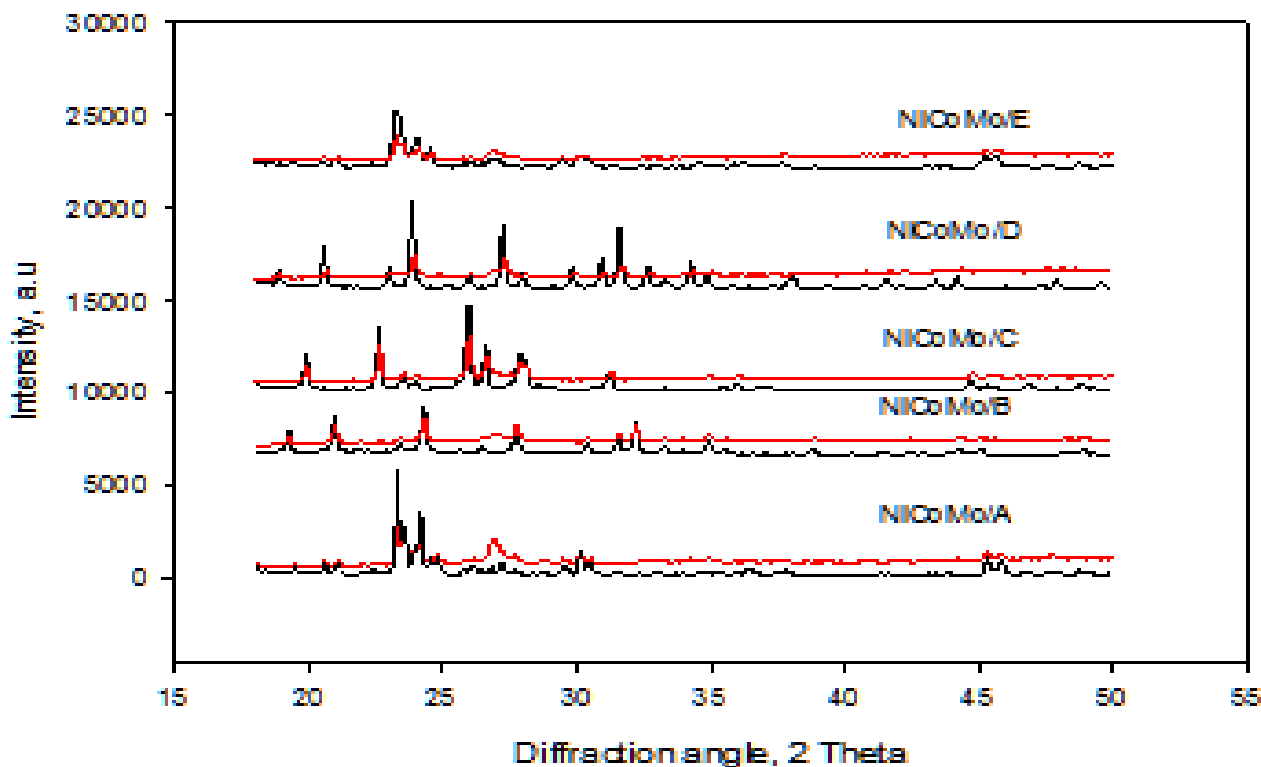


Fig.2: XRD patterns of the catalyst samples (A = ZSM-5a, B = HY-a, C = Mordenite, D = HY-b, E = ZSM-5b)

The Mo particles formed are of medium sizes which implies that there is fair dispersion of molybdenum inside the structure with a good metal-support interaction. Looi et al [18] observed a broad peak from the XRD patterns of molybdenum oxide supported over mesoporous alumina with small crystal sizes ranging from 2.09 to 5.44 nm. The absence of any peak attributed to nickel and cobalt in all the catalysts is an indication that they are well dispersed in the zeolite structure. In a similar work using NiO supported on ZSM-5 by Masalska [1], the characteristic diffraction lines attributable to NiO could not be detected in the final catalyst despite using metal loadings of 8%wt.

Table 4: Crystal size of the supported catalyst samples

Sample	crystal size of MoO ₃ , nm
NiCoMo/ZSM-5-a	20.43
NiCoMo/HY-a	20.43
NiCoMo/Mordenite	-
NiCoMo/HY-b	-
NiCoMo/ZSM-5-b	13.58

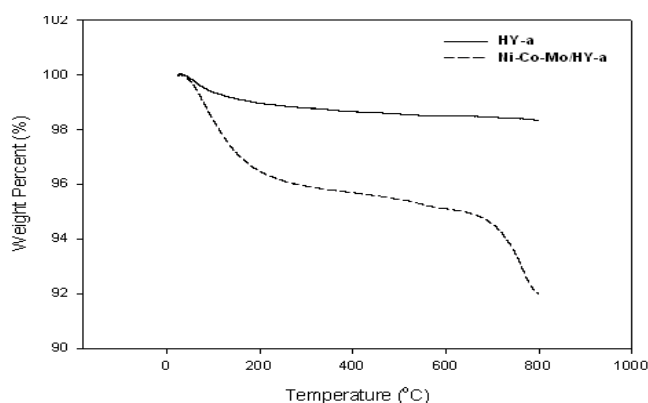
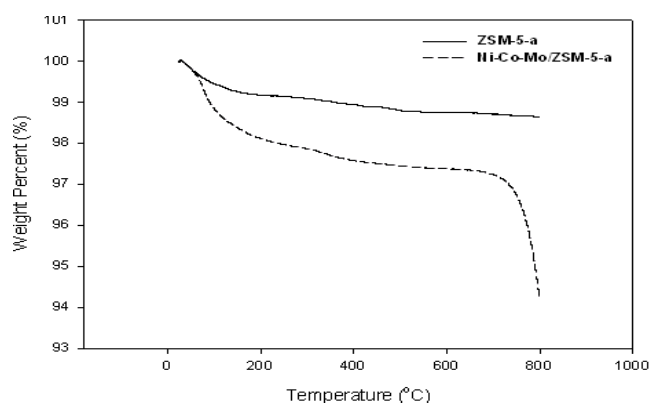
3.1.4 TGA/DSC Analysis

Figures 3 and 4 show the TGA and DSC curves for all the catalyst samples respectively. Each block gives the curves for the parent zeolite support and the zeolite-supported metal catalyst. According to the TGA curves, the first stage of decomposition starts with evaporation of water at 70-120 °C with about 2-6%wt loss. This is clearly shown in TGA curves in Fig.3. The impregnation of the metals on the zeolite supports slightly affected the thermal stability of the catalytic samples as shown in the figure. However, all the catalysts samples displayed thermal stability upto 730 °C. A phase transition started manifesting by a continuous loss in materials after this temperature for the supported metal catalyst samples while the support catalytic samples remained stable upto 800°C. The DSC curves (Fig. 4) show an endothermic transition for all the catalyst samples at 80-110 °C. This endotherm can be attributed to the evaporation of water physically

adsorbed on the catalysts surface (bulk water). The absence of glass transition indicates a pure crystalline material. Further heating of the catalyst samples did not display any peak which indicates stability in the absence of any heat effect.

3.1.5 Temperature-Programmed Reduction (Tpr)

The TPR profiles of the zeolite-supported metal catalytic samples are presented in Fig.5. The absence of peaks at lower temperatures (200-350 °C) is an indication that the metal salts used for the impregnation must have been reduced to their oxide forms after calcining. The appearance of first reduction peak (T_{red}) as shown in Fig.5 depends on the support material used with T_{red} - ZSM-5-a (555 °C) > HY-a (489) > ZSM-5-b (486) > Mordenite (476) > HY-b (446). This order also gives a hint on the support-metal interaction, in which the sample with the lowest reduction temperature (HY-b in this case) is expected to show high metal-support interaction. These reduction peaks which appeared at a temperature range (446 – 555 °C) for all the catalytic samples can be attributed to the reduction of MoO₃ supported on the zeolites[22]. Also as regards to the reduction temperature, it is worthy to note that NiCoMo/mordenite and NiCoMo/HY-b exhibited a significantly low-temperature reduction than the other three catalysts. This shift in reduction temperature can be linked to their large pore diameter which can enhance dispersion of the metal oxides and leads to reduction at comparatively lower temperature[23]. The shoulder peak observed at a reduction temperature of 500 °C for NiCoMo/HY-b can be attributed to either another specie of MoO₃ that weakly interacted with the support HY-b [22] or it is as a result of reduction of nickel (ii) oxide (NiO) in the catalyst [24]. Additional peaks were observed at high temperatures (680 – 780 °C) (see Fig. 5) which can be attributed to the reduction of divalent cobalt oxide to the metallic cobalt[6, 23].



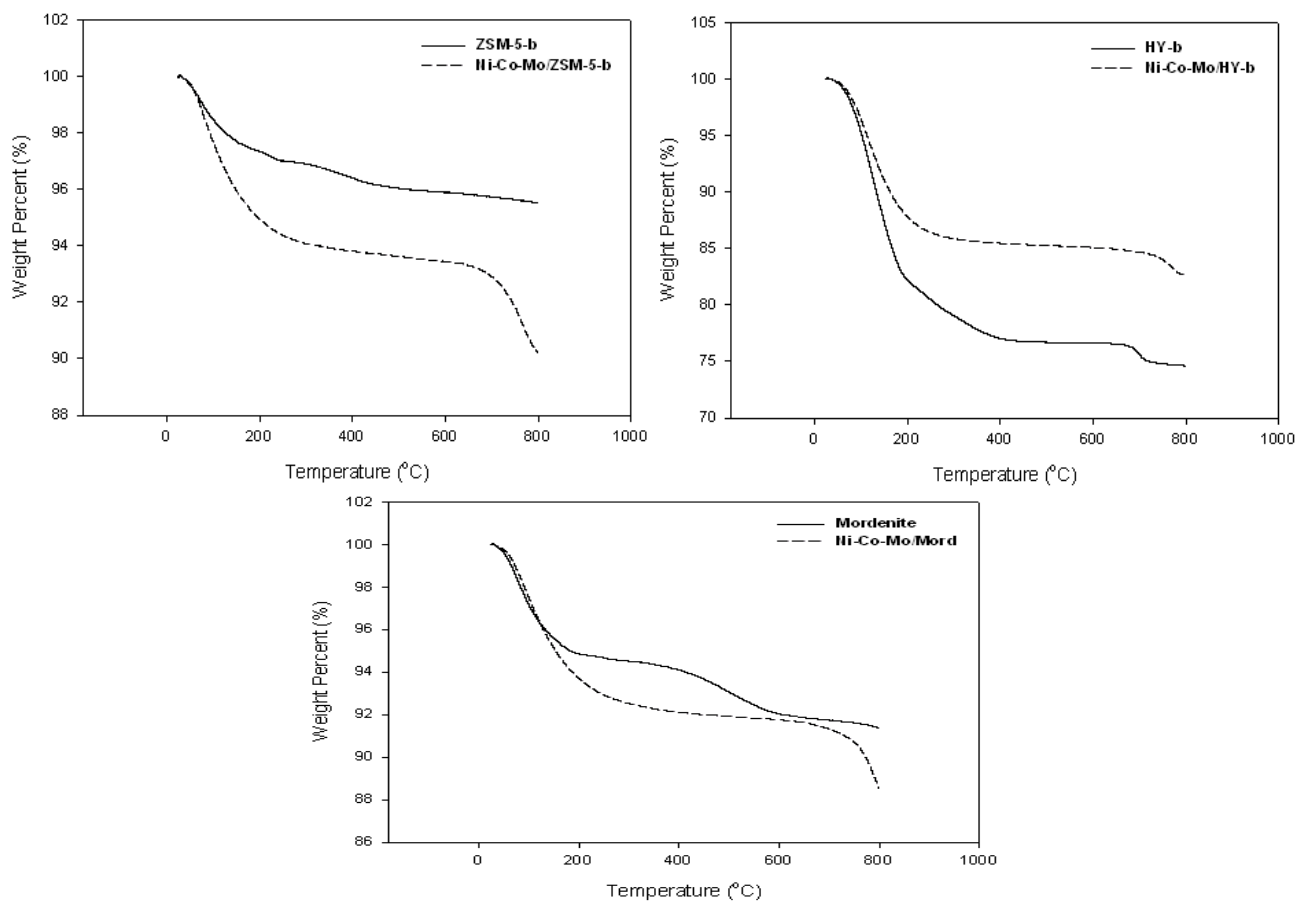
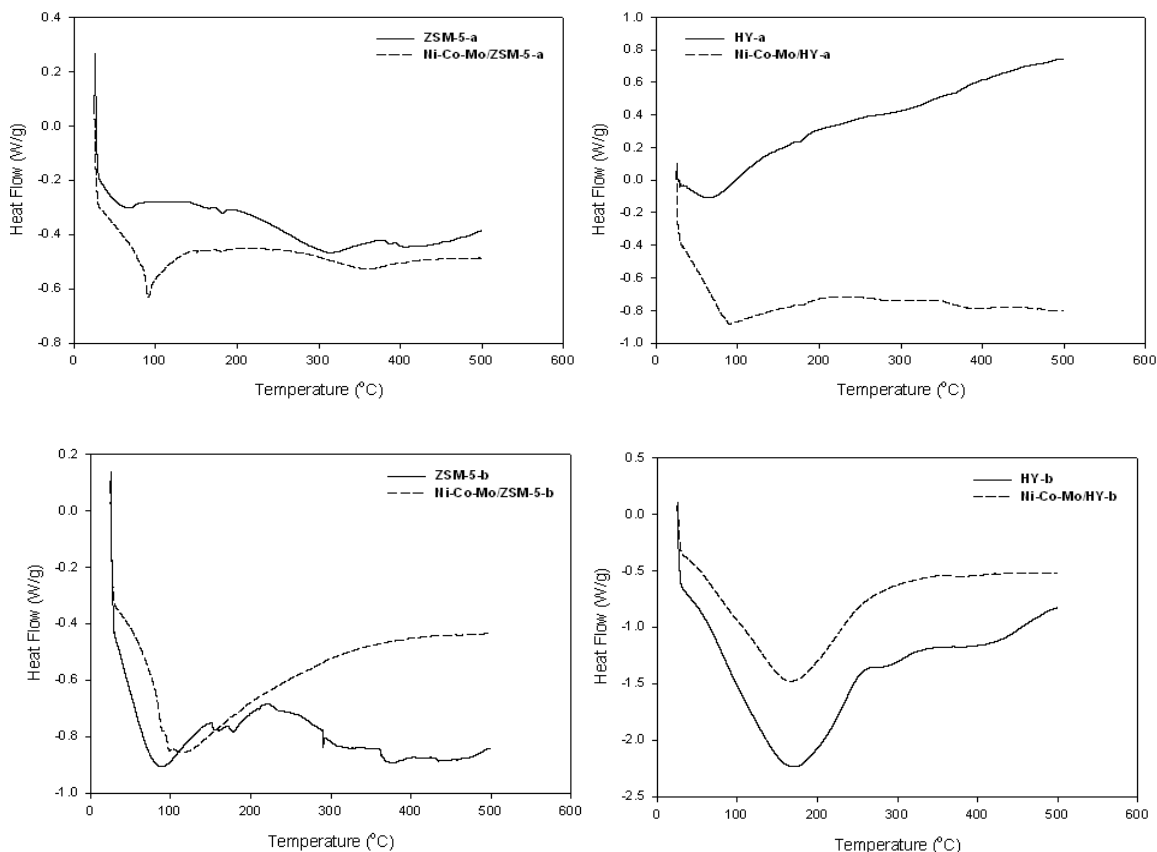


Fig. 3: Results from the TGA of the catalyst samples; each plot represents two samples i.e. zeolite support and the zeolite-supported metal catalyst



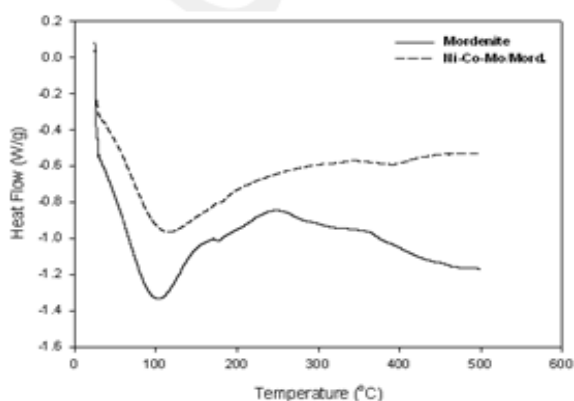


Fig. 4: Results from the DSC analysis of the catalyst samples; each plot represents two samples i.e. zeolite support and the zeolite-supported metal catalyst

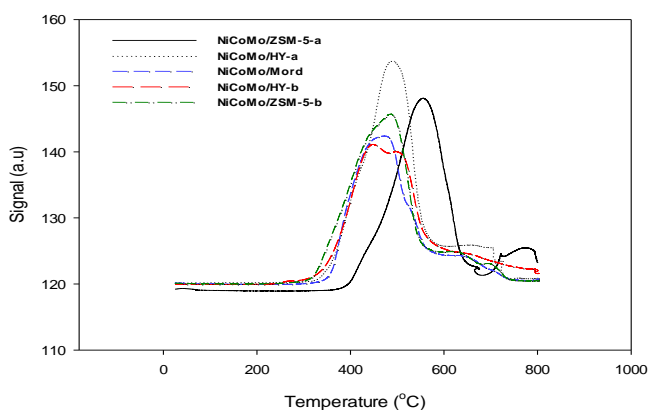


Fig.5: TPR profiles of the zeolite-supported metal catalytic samples

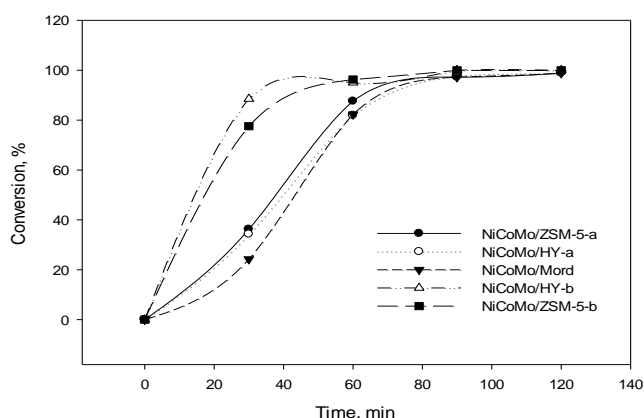


Fig. 6: A plot of conversion against time for the supported catalysts samples at 200°C

3.2 Catalyst Performance Evaluation

The toluene hydrogenation reaction yielded methylcyclohexane as the main product with traces of ethylcyclopentane in some of the catalysts systems tested. The conversion of toluene and selectivity of

ethylcyclopentane were calculated using equation (2) and (3) respectively.

$$\text{Conversion (\%)} = \frac{Tol_{initial} - Tol_{final}}{Tol_{initial}} \times 100 \quad (2)$$

$$\text{Selectivity (\%)} = \frac{MCH}{MCH + ECP} \times 100 \quad (3)$$

Where, Tol_{initial} is the initial concentration of toluene, Tol_{final} is the final concentration of toluene in the product stream, MCH is the concentration of methylcyclohexane and ECP is the concentration of ethylcyclopentane

When the reaction was carried out in the presence of the zeolite supports (ZSM-5-a, HY-a, Mord, HY-b, and ZSM-5-b), no new products were observed as the conversion of toluene was zero for all the parent zeolite supports. The inertness of the zeolite supports may be as a result of the low temperature used (200°C) and reaction time (2h) since they are known to be good catalysts for hydrogenolysis and isomerization reactions. Close to 100(%) conversion of toluene was observed in all the impregnated catalysts after about 90(mins) of reaction time. Under this condition, all the catalysts tested displayed good activity in toluene hydrogenation.

Fig.6 shows the catalyst activities in terms of conversion with time. NiCoMo/HY-b proved to be more active than all other catalysts at the beginning of the reaction. Its conversion is around 88(%) after 30(mins) of contact with the feed. This may be attributed to the strong adsorption of toluene on the catalyst surface due to insignificant pore diffusion limitations because of its large pore diameter than the other catalysts. Its high surface area may also contribute to higher activity since no other side products were observed, eliminating the possibility of more side reactions leading to other products.

The conversion of toluene up to 200°C leads to the formation of MCH as the main product; implying only hydrogenation takes place. The metals used in this work are known for hydrogenation/hydrocracking reactions, but because most cracking reactions take place at predominantly higher temperatures (above 200°C), no cracking products were observed in all the catalysts. Similar work conducted on toluene hydrogenation at low temperatures (150–200°C) yielded methylcyclohexane as the only product of the reaction[1, 25, 26]. The difference in terms of conversion between NiCoMo/HY-b with other supported catalyst samples at low reaction time may be

connected to the textural properties of the parent support.

Three drawbacks were identified as responsible for change in activity when conducting reactions using metals impregnated on porous materials like zeolites as; thermodynamics, catalyst poisoning and diffusion limitations[1]. The latter may hold in this case as the average pore diameters of the two catalysts are larger than the other ones. Thus, they are expected to have low resistance to pore diffusion when compared to others. The former may not be the case here as all other parameters are constant with a difference in only nature and type of support used. No any deactivation was noted throughout the length of time the reaction was conducted as there wasn't a drop in conversion. This is an indication that the catalysts were not poisoned in the course of this reaction.

When the reaction was repeated at 150°C using NiCoMo/HY-b, similar trend to 200°C was observed. The maximum conversion (100%) which was achieved after 90(mins) of reaction at 200°C was achieved here after 4.5h of reaction time (Fig. 7). This shows that toluene hydrogenation using this catalyst can be carried out at relatively lower temperature (150°C) but at longer reaction time. This is not a surprise as many researchers have reported toluene hydrogenation to be thermodynamically favored exothermic reaction.

The toluene hydrogenation reaction was repeated at a higher concentration (20% v/v of toluene in dodecane) over the NiCoMo/HY-b catalyst as shown in Fig. 8 below. NiCoMo/HY-b was used because of high activity it displayed when compared with other catalytic samples. Similar trend to the reaction at 150°C was observed with an only difference in the time (4h) the maximum conversion was reached and the product/products formed. However, methylcyclohexane was not the only product noticed in this reaction as small amounts of ethylcyclopentane; its isomer was observed in the product stream.

The toluene adsorbed on the catalysts surface can be hydrogenated by hydrogen adsorbed through two different mechanisms. Hydrogen adsorbed on the conventional metal active sites and the spillover hydrogen that migrates from the metal sites to the acidic sites. Production of methylcyclohexane from toluene by hydrogenation using metals is by carbonium ion theory.

The MCH carbonium ion formed on the metal active sites can be adsorbed on both the metal active sites and the acidic sites on the zeolite supports. This intermediate can be adsorbed on both Bronsted acid

site and Lewis acid site. However, Masalska, (2005) reported that Lewis acid sites, being electron-deficient, can easily adsorb aromatic molecules because of their π -bonds are electron donors[1]. But the electron-deficient aromatic intermediates like the MCH intermediate which form on these sites can be easily hydrogenated but difficult to isomerize.

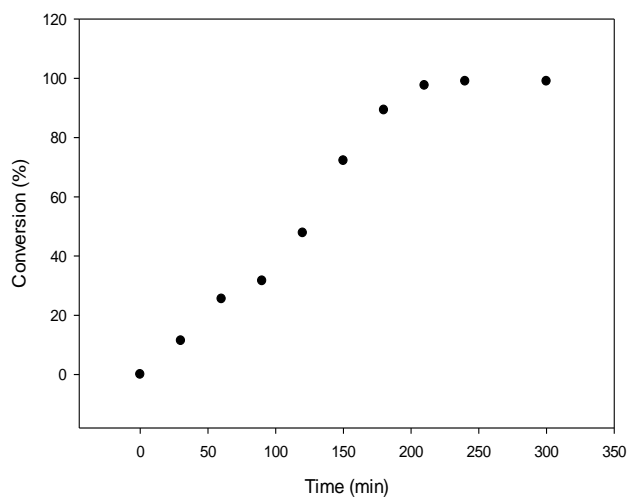


Fig. 8: Conversion against time for NiCoMo/HY-b with higher amounts of toluene at 200°C

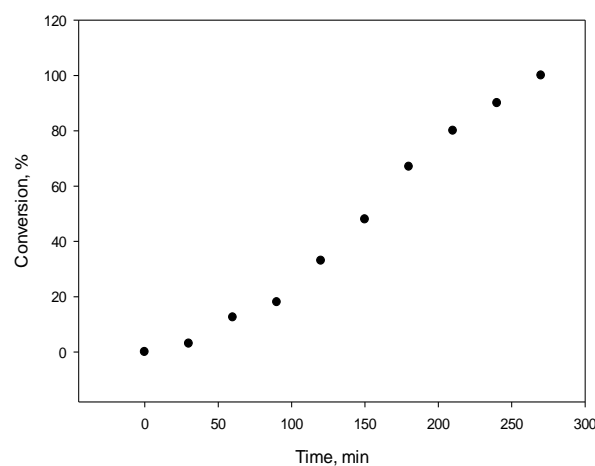


Fig. 7: Conversion against time for NiCoMo/HY-b at a lower temperature (150°C)

The large amounts of toluene used here and the high surface area of NiCoMo/HY-b may be responsible for the inability of the Bronsted acidic sites to hydrogenate the entire MCH carbonium ion adsorbed on its surface. Therefore, the MCH carbonium ions can be easily converted to ethylcyclopentane carbonium ions or its derivatives, and finally hydrogenate into ethylcyclopentane through isomerization and skeleton rearrangements. In a relevant work by (Thybaut *et al*, 2002[27]; hydrogenation of toluene on Pt/ZSM-22 yielded methylcyclohexane as the main product with small amounts (<5%) of ethylcyclopentane were

observed, while only trace quantities of dimethylcyclopentane isomers were found on the reactor effluent.

4. CONCLUSION

Trimetallic catalysts were prepared by impregnating three mixed metal oxides (Ni, Co, Mo) on five different zeolite supports. The catalysts were characterized by surface area and porosity measurements (BET), XRD, elemental analysis (ICP), TPR, TGA and DSC. XRD patterns for both zeolite supports and zeolite-supported metal catalysts showed that the framework of the zeolites were retained after the impregnation. Impregnation of the metals on the zeolites slightly affected their thermal stability as shown by the TGA/DSC analysis, although all catalysts displayed good thermal stability upto 730°C. XRD and TPR results confirmed the presence of molybdenum trioxide on the zeolites with NiCoMo/HY-b displaying high metal-support interaction due to low reduction temperatures. Mordenite and HY-b because of high pore diameter which enhances dispersion of the metal oxide leads to reduction at relatively lower temperatures. Close to 100% conversion to mainly methylcyclohexane was achieved. When the concentration of the reactant was increased using NiCoMo/HY-b, trace quantities of ethylcyclopentane was observed in the product stream. Under the reaction conditions studied and using the zeolite supports as catalysts no new products were observed.

The catalyst's activity tests conducted using toluene as a model compound showed that the support textural properties particularly surface area, pore volume and pore diameter affect the performance of the catalysts. NiCoMo/HY-b displayed the best performance after the few minutes of the reaction due to its high surface area, pore volume and average pore diameter. All the zeolite-supported metal catalysts gave excellent result in hydrogenation of toluene (with about 100% conversion after 90mins of reaction) and are proved effective catalysts for that purpose.

5. ACKNOWLEDGEMENTS

The authors would like to thank The Research Council of Oman for providing financial support to this work through the research grant; RC/ENG/PCED/11/01. The authors are also grateful to Centre for Theory and Applied Catalysis of the School of Chemistry and Chemical Engineering, Queens University of Belfast, UK for giving access to their research facilities to conduct the activity test and analytical techniques.

6. REFERENCES

- [1] Masalska, A. "Ni-loaded catalyst containing ZSM-5 zeolite for toluene hydrogenation," *Applied Catalysis A: General* 294, pp. 260-272, 2005.
- [2] Frauwallner, M., Lara-Romero, J., Scot, C. E., Ali, V., Hernandez, E., and Pereire-Almao, P. "Toluene hydrogenation at low temperature using a molybdenum carbide catalyst," *Applied Catalysis A: General* 394, pp. 62-70, 2011.
- [3] Loiha, S., Katrin-Zorn, K. F., Klysubun, W., Ruppachter, G., and Wittayakun, J. "Catalytic enhancement of platinum supported on zeolite beta for toluene hydrogenation by addition of palladium," *Journal of Industrial and Engineering Chemistry* 15, pp. 819-823, 2009.
- [4] Chupin, J., Gnep, N. S., Lacombe, S., and Guisnet, M. "Influence of the metal and of the support on the activity and stability of bifunctional catalysts for toluene hydrogenation," *Applied Catalysis A: General* 206, pp. 43-56, 2001.
- [5] Barrio, V. L., Arias, P. L., Cambra, J. F., Guemez, M. B., Pawelec, B., and Fierro, G. L. G. "Aromatics hydrogenation on silica-alumina supported palladium-nickel catalysts," *Applied Catalysis A: General* 242, pp. 17-30, 2003.
- [6] Cattenot, M., Geantet, C., Glasson, C., and Brysse, M. "Promoting effect of ruthenium on NiMo/Al₂O₃ hydrotreating catalysts," *Applied Catalysis A: General* 213, pp. 217-224, 2001.
- [7] Takema Wada, K. K., Murata, S., and Nomura, M. "Effect of modifier Pd metal on hydrocracking of polyaromatic compounds over Ni-loaded Y-type zeolite and its application as hydrodesulfurization catalyst," *Catalysis Today* 31, pp. 113-120, 1996.
- [8] Al-Saleh, M. A., Hossain, M. M., Shalabi, M. A., Kimura, T., and Inui, T. "Hydrogen spillover effects on Pt-Rh modified Co-clay catalysts for heavy oil upgrading," *Applied Catalysis A: General* 253, pp. 453-459, 2003.
- [9] Patricia Rayo, J. R., Torres-Mancera, P., Marroquin, G., Maity, S. K., and Ancheyta, J. "Hydrodesulfurization and hydrocracking of Maya crude with P-modified NiMo/Al₂O₃ catalysts," *Fuel*, pp. 1-9, 2012.
- [10] Koichi-Sato, Y. I., Yoneda, T., Nishijima, A., Miki, Y., and Shimada, H. "Hydrocracking of diphenylmethane and tetralin over bifunctional NiW sulfide catalysts supported on three kinds of zeolites," *Catalysis Today* 45, pp. 367-374, 1998.
- [11] Koichi Sato, Y. I., Miki, Y., and Shimada, H. "Hydrocracking of Tetralin over NiW/USY Zeolite Catalysts: For the Improvement of Heavy-Oil Upgrading Catalysts," *Journal of Catalysis* 186, pp. 45-56, 1999.

- [12] Ali, M. A., and Masuda, T. "Development of heavy oil hydrocracking catalysts using amorphous silica-alumina and zeolites as catalysts supports," *Applied Catalysis A: General* 233, pp. 77-90, 2002.
- [13] J Carolina-Leyva, J. A., Travert, A., Mauge, F., Mariey, L., Ramirez, J., and Rana, M. S. "Activity and Surface Properties of NiMo/SiO₂-Al₂O₃ catalysts for hydroprocessing of heavy oils," *Applied Catalysis A: General* 425-426, pp. 1-12, 2012.
- [14] Ancheyta, J., Rana, M. S., and Furimsky, E. "Hydroprocessing of heavy petroleum feeds: Tutorial," *Catalysis Today* 109, pp. 3-15, 2005.
- [15] Rana, M. S., Samano, V., Ancheyta, J. and Diaz, J. A. I. "A review of recent advances on process technologies for upgrading of heavy oils and residua," *Fuel* 86, pp. 1216-1231, 2007.
- [16] Hagen, J. "*Industrial Catalysis*", second edition, Germany: Weinheim, 2005.
- [17] van Santen, R. A., Moulijn, J. A., and Averil, V. A. *Catalysis: An Intergrated Approach*, Amsterdam: Elsevier, 2000.
- [18] Phaik-Yee-Looi, A. R. M., and Tye, C. T. "Hydrocracking of residual oil using molybdenum supported over mesoporous alumina as a catalyst," *Chemical Engineering Journal* 181-182, pp. 717-724, 2012.
- [19] Bin-Li, S. L., Li, N., Chen, H., Zhang, W., Bao, X., and Lin, B. "Structure and acidity of Mo/ZSM-5 synthesized by solid state reaction for methane dehydrogenation and aromatization," *Microporous and Mesoporous Materials* 88, pp. 244-253, 2006.
- [20] Emara, M. M., Medhat, A. S. M. T., and El-Moselhy, M. "Structural modification of mordenite zeolite with Fe for the photo-degradation of ZOTA," *Journal of Hazardous Materials* 166, pp. 514-522, 2006.
- [21] Dazhi-Zhang, S. A. I. B., and Chadwick, D. "n-Butanol to iso-butene in one-step over zeolite catalysts," *Applied Catalysis A: General* 403, pp. 1-11, 2011.
- [22] Liang Zhao, J. G., Xu, C., and Shen, B. "Alkali-treatment of ZSM-5 zeolites with different SiO₂/Al₂O₃ ratios and light olefin production by heavy oil cracking," *Fuel Processing Technology* 92, pp. 414-420, 2011.
- [23] Nowinska, A. W. A. I. K. "Propane oxydehydrogenation over transition metal modified zeolite ZSM-5," *Applied Catalysis A: General* 243, pp. 225-236, 2003.
- [24] Abdel-Gafar A Ali, L. I. A., Aboul-Fotouh, S. M., and Aboul-Gheit, A. K. "Hydrogenation of aromatics on modified platinum-alumina catalysts," *Applied Catalysis A: General* 170, pp. 285-296, 1998.
- [25] Desikan, A. N., Zhang, W., and Oyama, T. S. "The effect of acid-base properties of supported molybdenum oxide in propylene oxidation," *Journal of Catalysis* 157, pp. 740-748, 1995.
- [26] Byambajav, E., and Ohtsuka, Y. "Hydrocracking of asphaltene with metal catalysts supported on SBA-15," *Applied Catalysis A: General* 252, pp. 193-204, 2003.
- [27] Hossain, M., Al-Saleh, M., Shalabi, M., Kimura, T., and Inui, T. "Pd-Rh promoted Co/HPS catalysts for heavy oil upgrading," *Applied Catalysis A: General* 278, pp. 65-71, 2004.
- [28] Gallaraga, C. E., Scott, C. E., and Pereira-Almao, P. "Hydrocracking of Athabasca bitumen using ultra dispersed Ni-W-Mo catalysts," in *World Congress on Chemical Engineering*, Montreal, 2009.
- [29] Jessica, S. N., Henroth, F., Weber, C. C., Masters, A. F., and Maschmeyer, T. "Robust bimetallic Pt-Ru catalysts for the rapid hydrogenation of toluene and tetralin at ambient temperature and pressure," *Applied Catalysis A: General*, vol. 454, pp. 46-52, 2013.
- [30] Ishihara, A., Itoh, T., Nasu, H., Hashimoto, T., and Doi, T. "Hydrocracking of 1-methylnaphthalene/decahydronaphthalene mixture catalyzed by zeolite-alumina composite supported NiMo catalysts," *Fuel Processing Technology*, vol. 116, pp. 222-227, 2013.
- [31] Thybaut, J. W., Saeys, M., and Marin, G. B. "Hydrogenation Kinetics of Toluene on Pt/ZSM-22," *Chemical Engineering Journal*, vol. 90, pp. 117-129, 2002.